Full length article

Design of lightweight magnesium car body structure under crash and vibration constraints

Morteza Kiani [a], Imtiaz Gandikota [b], Masoud Rais-Rohani [b,c,]*, Keiichi Motoyama [b]

[a] *Engineering Technology Associates Inc. (ETA), MI 48084, USA*
[b] *Center for Advanced Vehicular Systems, Mississippi State University, MS 39762, USA*
[c] *Department of Aerospace Engineering, Mississippi State University, MS 39762, USA*

Abstract

Car body design in view of structural performance and lightweighting is a challenging task due to all the performance targets that must be satisfied such as vehicle safety and ride quality. In this paper, material replacement along with multidisciplinary design optimization strategy is proposed to develop a lightweight car body structure that satisfies the crash and vibration criteria while minimizing weight. Through finite element simulations, full frontal, offset frontal, and side crashes of a full car model are evaluated for peak acceleration, intrusion distance, and the internal energy absorbed by the structural parts. In addition, the first three fundamental natural frequencies are combined with the crash metrics to form the design constraints. The wall thicknesses of twenty-two parts are considered as the design variables. Latin Hypercube Sampling is used to sample the design space, while Radial Basis Function methodology is used to develop surrogate models for the selected crash responses at multiple sites as well as the first three fundamental natural frequencies. A nonlinear surrogate-based optimization problem is formulated for mass minimization under crash and vibration constraints. Using Sequential Quadratic Programming, the design optimization problem is solved with the results verified by finite element simulations. The performance of the optimum design with magnesium parts shows significant weight reduction and better performance compared to the baseline design.

1. Introduction

With the growing industrial development and reliance on fossil fuels, Green House Gas (GHG) emission has become a major problem. There are many sources for GHG including the emissions from passenger cars with internal combustion engines. In the United States, the Environmental Protection Agency (EPA) and the National Highway Traffic Safety Administration (NHTSA) issued a joint regulation in August 2012 [1]. This new regulation will be imposed on passenger cars in model year 2017 through 2025 to improve GHG and fuel consumption standards for cars. Based on this new regulation, the emission for combined cars and trucks has to be reduced from 243 g/mile in 2017 to 163 g/mile in 2025; moreover, the fuel economy must be improved from 36.6 mpg in 2017 to 54.5 mpg in 2025. However, carmakers have to design their products not only to fulfill the new regulations but also to remain in competition with peers. Regardless of different successful approaches to improve fuel economy such as fuel quality enhancement, development of high performance engines and

* Corresponding author. Present address: Bagley College of Engineering, P.O. Box 9544, Mississippi State, MS 39762, USA. Tel.: +1 662 325 2270; fax: +1 662 325 8573.
  E-mail address: masoud@ae.msstate.edu (M. Rais-Rohani).

Production and hosting by Elsevier

fuel injection system, weight reduction is one of the promising approaches as by 10% weight reduction in passenger cars, the fuel economy improves by as much as 6–8% [2].

Applications of lightweight materials not only bring the potential for carmakers to reduce the car weight but also simultaneously satisfy the new regulations of fuel economy and emissions. A few lightweight materials have been introduced in automotive industry such as aluminum, magnesium, and composite materials. According to Dieringa and Kainer et al. [3], magnesium is considered to be a frontrunner material among other lightweight materials. A magnesium car body structure with equal stiffness can be 60% or 20% lighter than steel or aluminum design, respectively [4]. According to Refs. [5,6], the average use of magnesium in cars has increased from 0.1% (1.8 kg) in 1995 to 0.2% (4.5 kg) in 2007 in the United States. The future vision for magnesium shows the use of this material in cars will increase by 15% (about 227 kg) by 2020 [7]. This study estimates 5.5 kg of average use of magnesium in the current body structure for the cars produced in the United States. This small application of magnesium shows the concerns of the carmakers about magnesium related challenges. Some of these challenges have been addressed in the USAMP's report such as cost effectiveness, poor corrosion, joining, and durability.

Prior works on the application of magnesium alloys in car body structure include Parrish et al. [8] where 22 steel parts were replaced with magnesium (AZ31) counterparts. This replacement combined with structural optimization saved 54.5 kg in weight while most of the crashworthiness characteristics of the new design remained similar to the baseline design. Logan et al. [9] show that magnesium body structure not only offers more than 40% weight reduction as compared to a conventional steel structure but it also significantly improves the structural performance.

In extending the prior research by Parrish et al. [8], this paper investigates weight reduction of a car by combining multidisciplinary design optimization and replacing the baseline steel with magnesium counterparts so that the crashworthiness and vibration characteristics of the new design can be improved or at least maintained similar to its baseline design. The design optimization is based on minimizing the mass as the objective function. In addition, the peak acceleration, intrusion distance, energy absorption, and the three fundamental frequencies are selected as the design constraints. The crash simulations are set up only for a subset of crash scenarios typically used in the automotive industry. Three most important crash scenarios, Full Frontal Impact (FFI), Offset Frontal Impact (OFI), and Side Impact (SI) are used in this study. Although, the combination of crashworthiness responses and vibration characteristics limits the minimization of mass, the contrast between rigidity for vibration and softening for crash responses addresses important considerations for magnesium application in car body structure. In addition, design optimization of the car body structure under two different criteria (crash and vibration) and specific details related to the computational modeling, response approximations, and optimization are presented and discussed.

2. Problem overview and optimization setup

Both crashworthiness and vibration design criteria of a full-scale Finite Element (FE) model of the 1996 Dodge Neon are considered. A set of 22 steel parts is selected depending on their influence on such properties as internal energy absorption and stiffness. These selected parts are replaced by magnesium alloy AZ31 to demonstrate the effect of material replacement on car weight reduction. The number of parts selected was twenty-two but due to symmetry in the design, the design variables were reduced to fifteen. Moreover, a multidisciplinary design optimization problem is set up for mass minimization of magnesium replaced parts with crashworthiness responses in three crash scenarios (FFI, OFI, SI) and vibration analysis responses as design constraints. The wall thicknesses of the selected parts were defined as the design variables. Internal energy absorption of the parts, intrusion distance of toe-board and dashboard, and the peak acceleration value were selected as the responses in crashworthiness study as well as the first three fundamental frequencies attributes obtained from the vibration analyses.

To study the effect of magnesium on structural stiffness, the single objective (SO) optimum design addressed by Parrish et al. [8] was selected for comparison. Fig. 1 shows those 22 steel parts which were considered to be replaced by magnesium alloy subjected to design optimization constraints which are extracted from the crashworthiness and vibration responses of the steel baseline. The constraints allow obtaining a lighter design without compromising the crashworthiness or vibration behavior of the baseline car model with steel parts. To facilitate this process, the design space was expanded by changing the bounds of design variables for magnesium replaced parts. To limit the overall computation effort, only 22 parts were selected for replacement by magnesium; however, should more parts be selected as design variables, more mass could be saved. The parts with darker shade shown in Fig. 1 are symmetric parts of the design.

Table 1 shows the specification for the selected parts at the steel baseline and the SO optimization design of Parrish et al. [8], and Table 2 shows the associated responses for the two baselines that are used as the design constraints in this study.

Mass minimization for the modified body structure is achieved by the optimization problem shown below.

$$
\begin{aligned}
\text{Min} \quad & f(\boldsymbol{x}) \\
\text{s.t.} \quad & g_i(\boldsymbol{x}) = R_i(\boldsymbol{x}) - R_i^b \leq 0; \quad i = 1, 8 \\
& g_i(\boldsymbol{x}) = R_i^b - R_i(\boldsymbol{x}) \leq 0; \quad i = 9, 14 \\
& 0.5\,\text{mm} \leq x_j \leq 8\,\text{mm}; \quad j = 1, 15
\end{aligned}
\tag{1}
$$

where $f(\boldsymbol{x})$ is the objective function defined as the total mass of the selected components; the $g_{1-8}(\boldsymbol{x})$ constraints represent the design constraints on the intrusion distances of toe-board, dash board for FFI and OFI, intrusion distance of door for SI and acceleration of B-Pillar in all three crash scenarios. These responses are required to be less than or equal to their baseline values. The $g_{9-14}(\boldsymbol{x})$ constraints impose limits on the internal
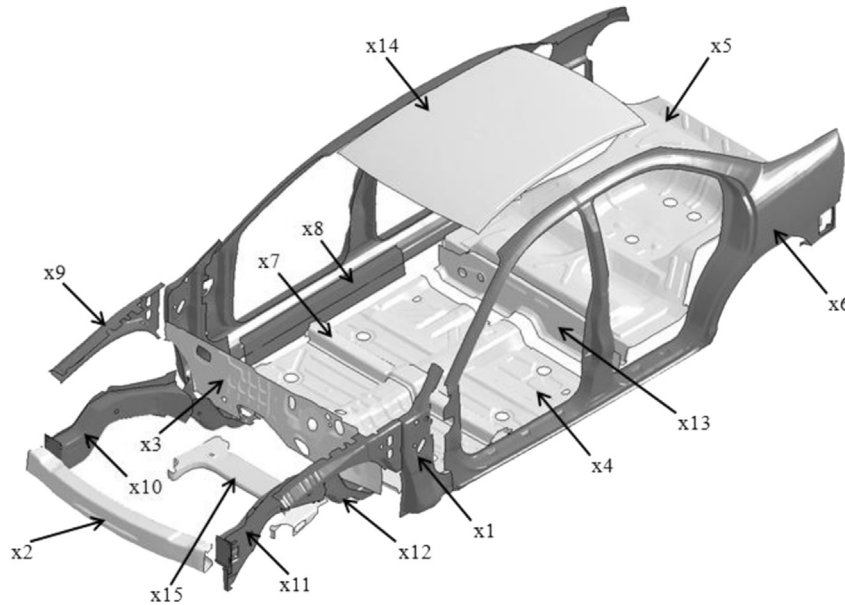
Fig. 1. Design variables and corresponding parts of 1996 Dodge Neon FE Model.

energies of selected parts in all three crash scenarios and also the first three fundamental frequencies of vibration analysis.

These responses are required to be greater than their baseline values because greater energy absorption decreases the risk of occupant injury and greater frequencies provide better structural rigidity and improve vibration characteristics of the car. The design variables were allowed to vary from 0.5 mm to 8 mm to find an optimum design. The subsequent sections of this paper discuss the material substitution process, FE models considered in crash and vibration analyses, type of surrogate models used, and solution of the optimization problem with results discussed at the end of the paper.

Table 1
Part specification and thickness of steel baseline and magnesium baseline addressed by Ref. [8].

Design variable	Component	Part no. in LS-DYNA	Steel baseline (mm)	Ref. [8] (mm)
1	A-Pillar	2000310,11	1.611	2.561
2	Front bumper	2000330	1.956	2.987
3	Firewall	2000352	0.735	0.867
4	Front floor panel	2000353	0.705	1.211
5	Rear cabin floor	2000354	0.706	0.569
6	Outer cabin	2000355,56	0.829	1.482
7	Cabin seat reinforcement	2000357	0.682	1.649
8	Cabin mid rail	2000358,59	1.050	1.792
9	Shotgun	2000373,74	1.524	1.810
10	Inner side rail	2000389,91	1.895	3.436
11	Outer side rail	2000390,92	1.522	3.145
12	Side rail extension	2000398,99	1.895	4.805
13	Rear plate	2000415	0.710	1.559
14	Roof	2000416	0.702	0.739
15	Suspension frame	2000439	2.606	4.367

3. Baseline design and response analysis

3.1. The FE crash model

The finite element crash simulation for the steel baseline design was performed and checked for accuracy using a publicly available, full-scale 1996 Dodge Neon car model developed by the National Crash Analysis Center (NCAC) [10]. Finite element crash simulations were performed for three crash scenarios involving FFI, SI and OFI using LS-DYNA [11] FE software. The simulations were set up for crash impact speeds, locations and angles as defined by the Federal Motor Vehicle Safety Standards (FMVSS) [12].

Fig. 2 shows the NCAC Dodge Neon FE model and multiple impact scenarios. The FE model consists of a total of 336 parts with 270,768 elements. Since the model does not contain interior parts (such as seats, steering wheel, occupant restraint system, instrument panel, etc.), total of 336

Table 2
Responses associated with different baseline models.

Response	Steel baseline	Ref. [8]
FFI Toe Int, mm	157.07	261
FFI Dash Int, mm	122.06	165
FFI Accel, g's	63.51	51
FFI Int eng, kJ	62.31	61
SI Door Int, mm	313.93	423
SI Accel, g's	47.88	40
SI Int eng, kJ	22.37	21
OFI Toe Int, mm	273.48	352
OFI Dash Int, mm	246.94	268
OFI Accel, g's	35.02	38
OFI Int eng, kJ	39.42	39
Frq1, Hz	35.39	32.74
Frq2, Hz	36.23	33.33
Frq3, Hz	38.37	35.42
Mass, kg	105.25	37.2

concentrated mass elements are distributed throughout the car to maintain the total mass of 1333 kg as in the actual crash test car. The majority of elements are modeled using Belytschko-Tsai element formulation (ELFORM 2) of LS-DYNA, and piecewise linear plasticity material model (MAT024) is considered for most of the parts in the baseline design.

The FE model does not include occupant models; therefore, acceleration measured at the top of B-Pillar is used to estimate the occupant injury according to the literature [8,13,14]. The FFI simulation was carried out at a speed of 56 km/h as specified by the U.S. New Car Assessment Program (NCAP), which is part of the FMVSS. The car collides with a flat rigid barrier consisting of 36 load cells modeled per NCAP guidelines. The SI crash involved a moving deformable barrier impacting the car on the driver side with a speed of 52.5 km/h at an angle of 27° with the lateral axis of the FE model. In OFI simulation, the Neon FE model crashes into a honeycomb block attached in front of a rigid barrier simulating another car located at 40% offset relative to car centerline. The FE crash simulations for all impact scenarios were carried out for a duration of 150 ms.

The crash behavior of the FE model in each crash scenario was partially validated by comparing the general trend of acceleration curves of test data and FE model, measured at accelerometers located at the left rear seat cross member for FFI, left rear sill for OFI and at middle of driver side B-pillar for SI [15−17]. Fig. 3 shows the comparison of acceleration curves of test and FE model. The FE model acceleration curves were filtered using a 60 Hz Butterworth filter to eliminate noise from the data, and this filtering scheme agrees with the type of filtering scheme used in the test data. The acceleration curves extracted from the simulations and tests are in reasonably good agreement.

In this paper, the most important crash responses, which are related to crashworthiness study, have been extracted for the three impact scenarios. The Internal Energy (IE) absorption is considered to be one of those important responses. Moreover, the intrusion distances of car toe-board (FFI_Toe and OFI_Toe), dashboard (FFI_Dash and OFI_Dash), and door (SI_Door), and acceleration at upper B-Pillar in all three scenarios (FFI_Acc, OFI_Acce, SI_Acc) were considered as substitutes for the responses associated with occupant safety metrics.

The acceleration at upper B-Pillar was measured by taking the average of the total acceleration values of 20 nodes that were selected as an approximate location of where the occupant head would be in actual crash. This helps improve the accuracy of the acceleration for development of the surrogate response models. The intrusion distances were measured by averaging the relative displacement of 20 nodes selected on toe-board, dashboard and door sites compared to an associated
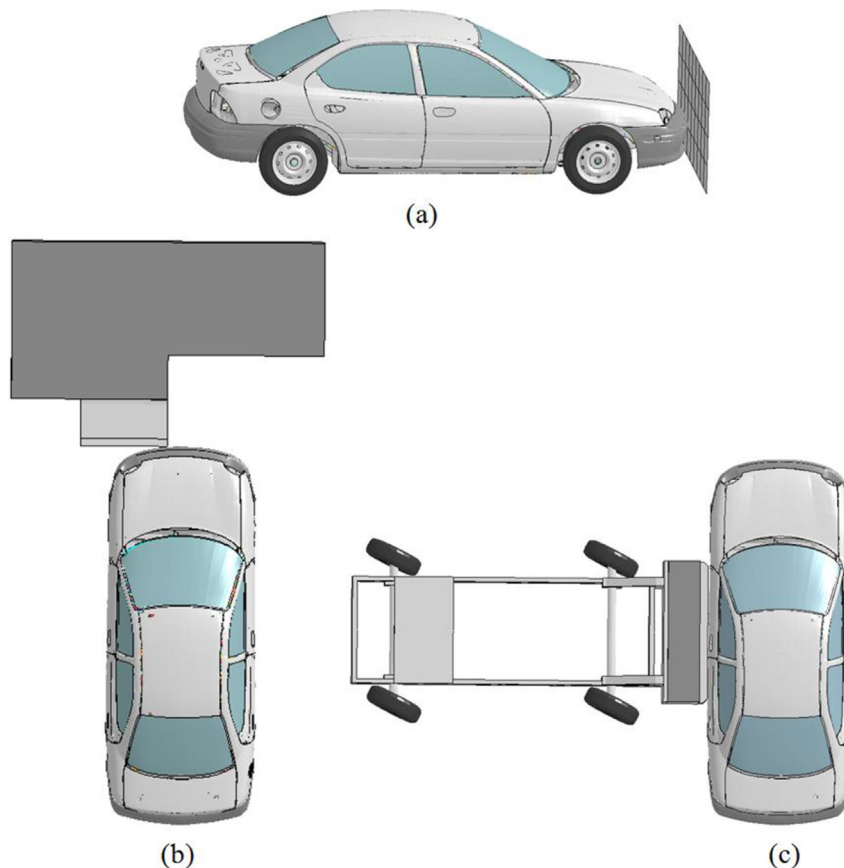

Fig. 2. Crash FE models of the 1996 Dodge Neon and setup for (a) FFI, (b) OFI, and (c) SI.
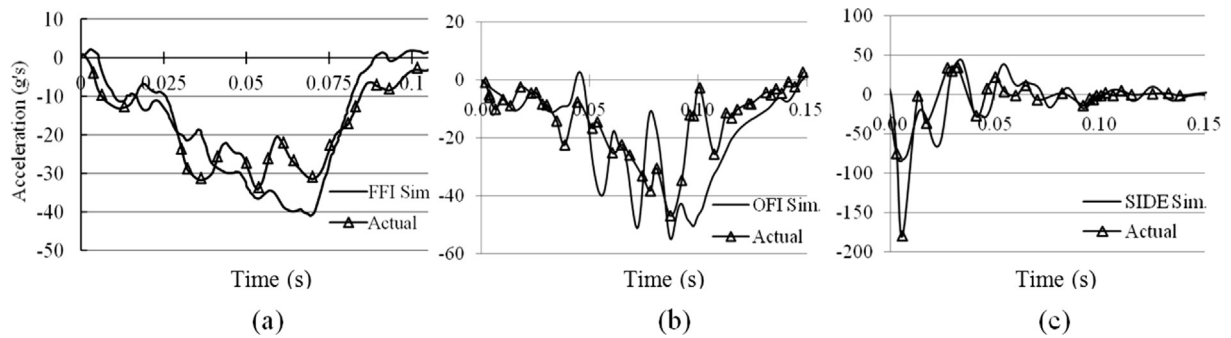
Fig. 3. Acceleration curves for (a) *x*-dir. FFI, (b) *x*-dir. OFI, and (c) *y*-dir. SI.

reference node such that the reference node does not exhibit deformation. Fig. 4 shows the locations for measuring intrusion distances and accelerations, few parts were removed to ease viewing.

3.2. The FE model of car for vibration analysis

Consideration of only the crashworthiness characteristics of a car limits the scope of car design and hinders the ride quality of the car. Noise, Vibration and Harshness (NVH) analysis helps improve the vibration attributes of designed cars. Apart from crashworthiness, NVH attributes have been considered as important design factors in auto body structural design. Sobieszczanski-Sobieski et al. [18] performed optimization of automotive structures by considering NVH characteristics along with crash analysis; Kiani et al. [14] conducted a multidisciplinary optimization of a car by considering crash and vibration as the design constraints and studied the effect of the optimization of the car with and without vibration characteristics. Various other studies have shown the importance of considering NVH in the design problem [19−23]. According to Paramjot et al. [22], consideration of fundamental vibration frequencies of the Body-in-White (BIW) determines the NVH performance as well as the stiffness characteristics of the car. In this article, both crash and vibration analyses were used to

improve the design of the baseline car. By considering crashworthiness and vibration responses, the competition between rigidity for improving the vibration characteristics of the car body structure and deformability necessary for improvement of energy absorption is included in the car design.

The FE model of 1996 Dodge Neon car used in the crash analysis cannot be used for performing modal frequency analysis due to various types of connections and parts involved in the model. Therefore, a vibration model of the car must be developed. The FE model used in crashworthiness study was modified to accommodate its use in MSC Nastran to conduct modal analysis. The FE model considered in vibration analysis did not contain any moving parts such as doors, hood, etc. but windshield and rear window were taken into account and all the spotwelds used in crash model were modified to have a better representation of the overall structural stiffness. The vibration model consisted of all the sheet metal components representing a BIW model, with components connected to each other using spotwelds defined with a nominal diameter of 5 mm. The spotwelds were modeled using CWELD element with elastic properties being same as its steel counterparts. The CNRB constraints used in LS-DYNA were converted into RBE2 type of constraint in MSC Nastran. The final BIW FE model developed for modal analysis consisted of 273,760
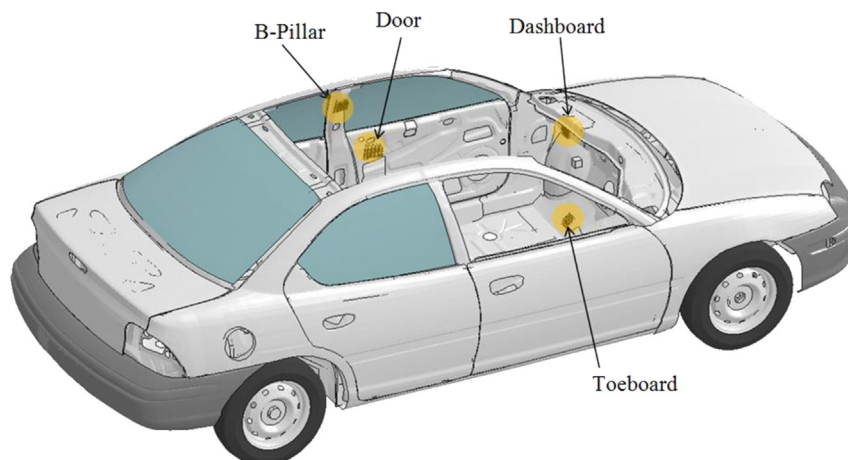

Fig. 4. Locations for measurement of intrusion distance and acceleration responses.

nodes, 262,560 CQUAD4 and CTRIA3 shell elements, 701 RBE2 and 3215 CWELD elements. Fig. 5 shows the developed BIW model such that the CWELD elements are scaled up and shown by solid spheres while the RBE2s are shown by open red circles.

Initially, the vibration model with steel parts was evaluated with responses being the first three fundamental frequencies associated with torsion, bending, and combined modes. The fundamental frequencies associated with the model were selected as evaluation metrics for structural rigidity which has a direct influence on NVH characteristics of a car [22].

4. Application of magnesium alloy in automotive structure

The growing interest in improving fuel efficiency has encouraged auto industry to come up with various techniques for obtaining a lighter design. One of the common techniques to achieve this demand is material replacement. This technique allows engineers to design a car body structure without compromising the safety and crashworthiness behaviors. Apart from this, research in lightweight materials such as magnesium alloys, lightweight alloy steels, aluminum and composite materials have allowed engineers to develop a lighter car design with improved crashworthiness and ride quality. Compared to aluminum and steel, magnesium shows better specific stiffness and specific strength [24]. Nevertheless, the poor creep behavior and low strength exhibited by magnesium at elevated temperatures should be resolved to facilitate the use of magnesium for car body structures.

To study the weight reduction, AZ31 was selected as a substitute material for steel, assuming that the process involved in manufacturing the parts is sheet forming. It has been experimentally observed that at room temperature, the stress-strain behavior of AZ31 alloys shows high yield strength and less elongation. Hence, the formability characteristics and anisotropic behavior of AZ31 are poor at room temperature but are better at elevated temperatures [25]. Moreover, the difference in anisotropic deformation is responsible for magnesium alloys having different failure points in tension and compression coupon tests.

To substitute magnesium alloy AZ31 for selected steel parts of the baseline model, material model MAT124 [26] in LS-DYNA was used, which is based on the model developed by Wagner et al. [27]. This model is believed to distinguish both tensile and compressive behavior of the material with the help of piecewise linear isotropic hardening model that is observed in magnesium stress-strain data. The stress-strain behavior of magnesium is highly sensitive to material anisotropy and strain rate, but the anisotropic behavior of alloys is less noticeable at higher strain rates. The material anisotropic behavior and its effect were neglected in defining the properties of MAT124 model. Since magnesium alloys are strain rate sensitive, the effects of strain rate in MAT124 model were considered through Cowper—Symonds model capable of scaling the yield stress as shown in Eq. (2).

$$\frac{\sigma_{0d}}{\sigma_0} = 1 + \left(\frac{\dot{\varepsilon}}{C}\right)^{\frac{1}{P}} \tag{2}$$

where σ_{0d} and σ_0 respectively, define the yield stress in dynamic impact and quasi-static compression loading, P and C are the Cowper—Symonds' coefficients for strain rate sensitivity, and $\dot{\varepsilon}$ is the strain rate.

In the above equation, parametric values $P = 3.09$ and $C = 24,124$ were selected and maintained the same for both tension and compression as described in literature [28]. Experimental data were used to define stress-strain curves of AZ31 under tension and due to unavailability of compression data, the ratio of stress-strain curves of AM30 magnesium alloy under compression and tension were multiplied times the tension data of AZ31 to obtain compression data of AZ31 [8]. The material failure can be determined by the failure strain limit which is the same for both tension and compression curves, but the material considered in this study had a higher tensile failure strain than compression. To avoid this difference, a material softening procedure was implemented in compression curve. Material substitution was performed by defining the MAT124 material properties for the selected parts. These selected parts had different steel properties before material replacement, but for the design with magnesium, the same properties were used in assigning the material model.
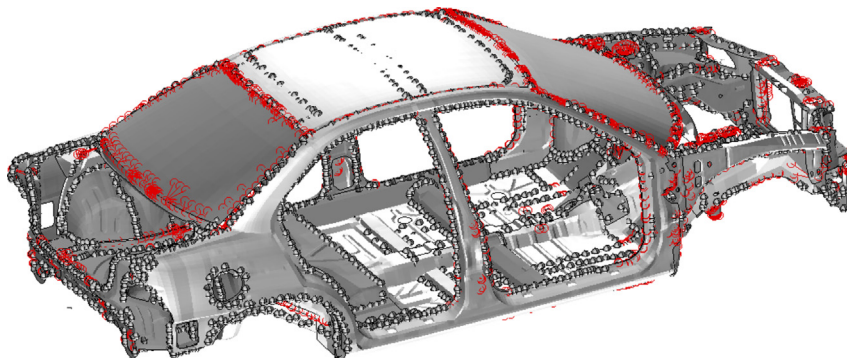

Fig. 5. Vibration FE model of the 1996 Dodge Neon.

5. Response approximation and optimization setup

5.1. Surrogate modeling

The computational time for performing crash simulation depends on the crash scenario and the computing capabilities and performance of the computer system used. Using a high performance computer system equipped with four six-core processors for vibration analysis takes at least 1 CPU hour whereas one single crash simulation for FFI, OFI, and SI takes up to 3, 12, and 8 hours, respectively. In optimizing a design, the optimizer calculates the responses at various values of the design variables within the prescribed bounds. To facilitate this process, direct interaction of optimizer with simulation software is not feasible because of the time involved in running each simulation. To eliminate the extra computation cost associated with running of simulations at each design point, the required responses are transformed into a set of mathematical models or analytical functions known as surrogate models, which are approximate functions of the actual response built with the help of design of experiments (DOE) technique [29–34]. Using surrogate models helps optimization of systems that involve noisy responses [35]. The responses obtained in a crash analysis are highly nonlinear and noisy; hence, the selection of an appropriate type of surrogate model is crucial to have better approximations. There are different types of surrogate models such as Radial Basis Function (RBF), Kriging (KG), and Polynomial Response Surface (PRS), etc. The choice and accuracy of the surrogate model depends on the type of response and the number of design points used to build the models.

There are different methods for selecting the design points used in surrogate model construction, such as Latin Hypercube Sampling (LHS), Taguchi Orthogonal Array, etc. In this paper, LHS was used to generate the design points scattered throughout the design space as specified by the upper and lower bounds of the design variables. Once the design points obtained through LHS were evaluated using actual simulations, RBF technique was used to build the surrogate models. The RBF technique develops a relationship between design variables and responses based on the Euclidean distance using linear combinations of radially symmetric functions. The general form of RBF is given as

$$\widehat{f}(\mathbf{y}) = \sum_{k=1}^{N} \lambda_k \phi(\|\mathbf{y} - \mathbf{y}_k\|) = \sum_{k=1}^{N} \lambda_k \phi\left(\sqrt{(\mathbf{y} - \mathbf{y}_k)^T (\mathbf{y} - \mathbf{y}_k)}\right) \quad (3)$$

where ϕ is the type of basis function defined based on:

1 − thin plate spline: $\phi(r) = r^2 \ln(c\,r)$, 2 − Gaussian: $\phi(r) = \exp(-c\,r^2)$, 3 − multiquadric: $\phi(r) = \sqrt{r^2 + c^2}$, and 4 − inverse multiquadric: $\phi(r) = 1/\sqrt{r^2 + c^2}$, with $0 \le c \le 1$ and r representing the normalized radial distance.

The RBF surrogate model is very sensitive to the choice of basis function and the value of parameter c. The coefficient λ_k, is obtained by fitting the surrogate model using the points of DOE also called as training points. The surrogate models were built and the combination of basis function with parameter c

was checked for accuracy using a few test points for each response surrogate model. The surrogate models were generated based on 138 training points, and the error calculation showed permissible error level for each response.

5.2. Surrogate-based optimization and the results

The surrogate models as discussed in the last section were used to formulate response functions and were treated as design constraints. Mass was considered as the objective function and wall thickness of the selected 22 parts were treated as the design variables. A relation between wall thickness of baseline model and mass of the associated parts were used to determine the new mass of the parts. Steel baseline design responses were considered as design constraint bounds. The optimum design obtained by material replacement must have better or at least similar performance as the steel design with an added advantage of being a lighter design. The design optimization problem stated in Eq. (1) was solved using optimization toolbox available in MATLAB [fmincon].

Sequential quadratic programming (SQP) was used as an optimization method. SQP is a gradient-based optimization technique and the total time it takes to find the optimum point is less as compared to gradient free methods. Since SQP is a local optimizer, different initial design points were used to arrive at different local optimum points in the design space for finding the best results. The optimization process for the best case took a total of 76 iterations with 2133 function calls. A single iteration in SQP method involves the calculation of a quadratic sub-problem, updated step size and search direction. The change in the objective function with respect to iterations is shown in Fig. 6. The mass of 22 parts with steel design was 105.23 kg and after material substitution and design optimization, the mass reduced to 58.52 kg indicating a reduction of 44.3% of mass. Table 3 shows the optimum wall thickness of the selected parts found in this study along with steel baseline and design proposed by Parrish et al. [8].

Fig. 7 corresponds to the values of normalized design variables for steel baseline, SO optimum design proposed by Parrish et al. [8], and current optimum results. The optimum responses predicted by surrogate models were checked for accuracy by performing FE simulation of the predicted design. Table 4 shows the error associated with the surrogate model responses by comparing to the actual simulation results. The average error for all the responses is 4.78%.

Table 5 shows the comparison of results obtained with material substitution, by including both crash-vibration design criteria versus crash alone design developed in Ref. [8]. It can be demonstrated that by considering steel baseline responses as constraints, better crash behavior can be obtained in the design. Moreover, it can be seen that even after replacing the steel parts with magnesium, the intrusion distances have been maintained within the acceptable limits, and vibration characteristics defined by frequency responses have improved compared to the steel baseline design. Even though magnesium is lighter, by using optimization techniques the overall stiffness has been improved by tuning the frequency
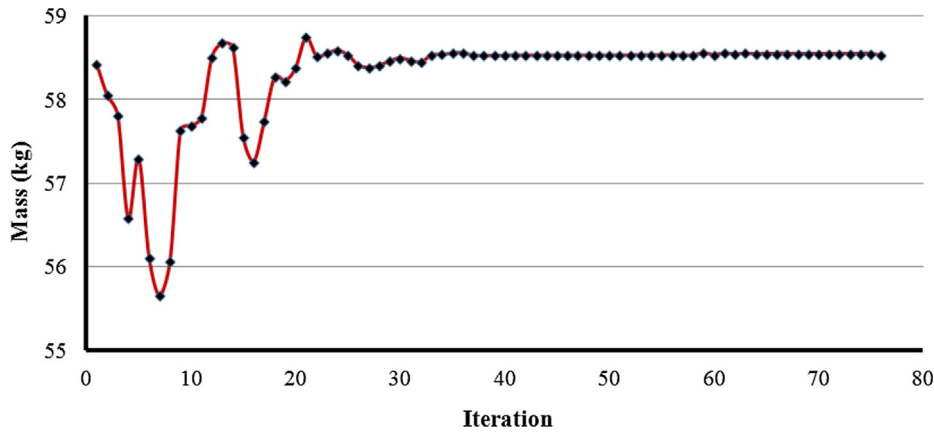
Fig. 6. Change in objective function with respect to iteration.

Table 3
Thickness of the parts in the baseline, Ref [8], and current optimum design.

Design variable	Component	Steel Baseline, mm	Ref. [8], mm	Current Optimum design, mm
1	A-Pillar	1.611	2.561	2.004
2	Front bumper	1.956	2.987	5.639
3	Firewall	0.735	0.867	1.742
4	Front floor panel	0.705	1.211	2.341
5	Rear cabin floor	0.706	0.569	0.519
6	Outer cabin	0.829	1.482	3.323
7	Cabin seat reinforcement	0.682	1.649	2.653
8	Cabin mid rail	1.050	1.792	1.353
9	Shotgun	1.524	1.810	3.393
10	Inner side rail	1.895	3.436	3.696
11	Outer side rail	1.522	3.145	3.276
12	Side rail extension	1.895	4.805	2.765
13	Rear plate	0.710	1.559	2.075
14	Roof	0.702	0.739	1.711
15	Suspension frame	2.606	4.367	4.520

responses. Moreover, the results obtained for accelerations and internal energies indicate that the accelerations and overall internal energy absorption of the parts have been improved as compared to the steel baseline design. To have better internal energy absorption, the resulting structure should be soft and magnesium can offer a desirable soft structure.

It is evident from Table 5 that by considering steel baseline model responses as the design constraints, there is considerable amount of weight reduction without compromising the crashworthiness behavior of the car. This is indicated by reduction in intrusion distances of two different optimized magnesium designs. The first three fundamental frequencies from Table 5 indicate that considering crash responses only as design constraints, decreases the overall stiffness of the car. Including vibration requirements along with crash in the design with magnesium parts increased the mass. However, a better design with improved crashworthiness behavior and structural rigidity can be obtained compared to the steel baseline design.
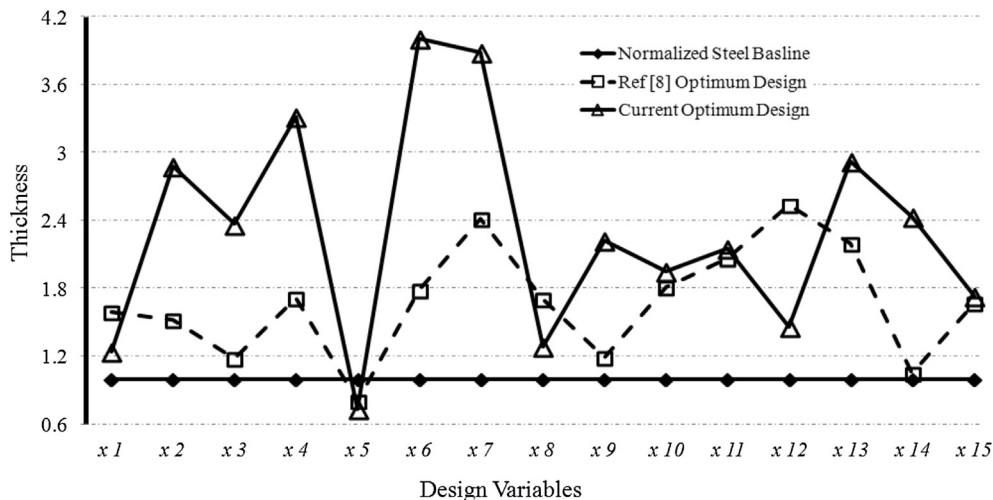

Fig. 7. Normalized optimum part thicknesses for different design cases.

Table 4
Comparison between surrogate responses with actual simulation results.

Response	Surrogate-based value	FE-based value	Difference (%)
FFI Toe Int, mm	150.1	152.33	−1.5
FFI Dash Int, mm	92.5	85.94	7.1
FFI Accel, g's	57.7	58.25	−0.9
FFI Int eng, kJ	64.3	63.27	1.6
SI Door Int, mm	298.1	296.71	0.5
SI Accel, g's	46.9	47.35	−1.1
SI Int eng, kJ	22.4	21.82	2.5
OFI Toe Int, mm	214.8	175.28	18.4
OFI Dash Int, mm	134.4	154.42	−14.9
OFI Accel, g's	34	37.28	−9.6
OFI Int eng, kJ	40.9	40.85	0.1
Frq1, Hz	35.3	36.02	−2.8
Frq2, Hz	36.2	38.33	−5.8
Frq3, Hz	39.6	39.21	0.9
Average error%			4.7

6. Conclusion

This study investigated the application of material substitution, surrogate modeling, and structural optimization techniques to develop a lightweight car design with improved structural performance. Total of 22 steel parts of the 1996 Dodge Neon car model were selected and replaced by magnesium AZ31. The wall thicknesses of the parts were selected as design variables and a structural design optimization problem was formulated with mass of the selected parts as the objective function. Crashworthiness and vibration responses of the FE model were treated as design constraints.

To obtain crashworthiness responses, the FE model of Dodge Neon was analyzed by LS-DYNA for three most important crash scenarios (FFI, OFI and SI). To include vibration design requirements, the full FE crash model of the car was modified to BIW model for compatibility with MSC NASTRAN vibration analysis. The first three fundamental natural frequencies were taken as responses of vibration analysis due to their effect on structural rigidity. Using LHS, 138 design points were generated and simulations were run to obtain corresponding responses. To reduce computation cost

Table 5
Comparison of optimum designs with baseline.

Response	Steel baseline	Ref. [8]	Current results
FFI Toe Int, mm	157.07	261	152.33
FFI Dash Int, mm	122.06	165	85.94
FFI Accel, g's	63.51	51	58.25
FFI Int eng, kJ	62.31	61	63.27
SI Door Int, mm	313.93	423	296.71
SI Accel, g's	47.88	40	47.35
SI Int eng, kJ	22.37	21	21.82
OFI Toe Int, mm	273.48	352	175.28
OFI Dash Int, mm	246.94	268	154.42
OFI Accel, g's	35.02	38	37.28
OFI Int eng, kJ	39.42	39	40.85
Frq1, Hz	35.39	32.74	36.02
Frq2, Hz	36.23	33.33	38.33
Frq3, Hz	38.37	35.42	39.21
Mass, kg	105.25	37.2	58.52

associated with computer simulations, surrogate modeling technique were used to approximate the responses at each training point.

A structural design optimization problem was solved using SQP technique to obtain an optimum design with reduced mass and improved crash and vibration behavior. The results obtained demonstrated that after material substitution and using the steel baseline responses as the design constraints, significant mass reduction was achieved in the optimum design without compromising crashworthiness and vibration characteristics of the vehicle. The additional consideration of vibration requirements in the problem improved structural rigidity as well as crashworthiness performance of the car. Substitution of magnesium alloy and design optimization resulted in an overall weight saving of 46.7 kg indicating an approximate mass reduction of 44.3% compared to the baseline steel design.

References

[1] Office of Transportation and Air Quality, Regulatory Announcement: EPA and NHTSA Propose to Extend the National Program to Reduce Greenhouse Gases and Improve Fuel Economy for Cars and Trucks, 2011. EPA-420-F-11-038.
[2] U.S. Department of Energy, Lightweighting Material: 2010 Annual Progress Report, 2011. DOE/EE-0577.
[3] H. Dieringa, K.U. Kainer, Mat-wiss U Werkst. 38 (2) (2007) 91−96.
[4] R. Porro, The Innovative Use of Magnesium in Car Design and An Analysis of Cost Versus Weight Savings, 1998. SAE Paper, 980084.
[5] R.A. Schultz, A.K. Abraham, in: Great Designs in Steel Seminar, American Iron and Steel Institute, Southfield, Mich, 2007.
[6] Ward's Communications, 2008. Ward's Motor Vehicle Facts and Figures 2008. Southfield, Mich.
[7] G.S. Cole, Magnesium Vision 2020: A North American Automotive Strategic Vision of Magnesium, 2007. USAMP report 2007.
[8] A. Parrish, M. Rais-Rohani, A. Najafi, Int. J. Crashworthiness 17 (2012) 259−281.
[9] S. Logan, A. Kizyma, C. Patterson, S. Rama, et al., Lightweight Magnesium Intensive Body Structure, 2006, http://dx.doi.org/10.4271/2006-01-0523. SAE Technical Paper 2006-01-0523.
[10] Finite Element Model of Dodge Neon: Model Year 1996 Version 7, 2006. Available at: http://www.ncac.gwu.edu/vml/archive/ncac/vehicle/neon-0.7.pdf.
[11] LS-DYNA Nonlinear Explicit Finite Element Software, Livermore Software Technology Corporation, Livermore, CA, 2007.
[12] NHTSA, Federal Motor Vehicle Safety Standard, U.S. Department of Transportation, National Highway Traffic Safety Administration, Washington, DC, 1998.
[13] J. Hurnall, A. Draheim, M. Case, J. Del Beato, et al., in: Proceedings of 18th International Technical Conference on the Enhanced Safety of Vehicles, Nagoya, Japan, 2003.
[14] M. Kiani, I. Gandikota, A. Parrish, K. Motoyama, M. Rais-Rohani, Int 18 (5) (2013) 473−482. J. Crashworthiness.
[15] NCAP, Frontal Barrier Impact Test: 1996 Dodge Neon, NCAP, Washington, DC, 1995. Prepared by Transportation Research Center Inc. for the U.S Department of Transportation.
[16] NHTSA, Frontal Barrier Forty Percent Offset Impact Test: 1996 Dodge Neon, NHTSA, Washington, DC, 1997. Prepared by Kargo Engineering for the U.S. Department of Transportation.

[17] MGA, Safety Compliance Testing for FMVSS 214 'Side Impact Protection – Passenger Cars: 1997 Dodge Neon, MGA, Washington, DC, 1997. Prepared by MGA proving Grounds for the U.S. Department of Transportation.

[18] J. Sobieszczanski-Sobieski, S. Kodiyalam, R.J. Yang, et al., Struct. Multidiscip. Optim. 22 (2001) 298–306.

[19] D.C. Lee, H.S. Choi, C.S. Han, et al., Struct. Multidiscip. Optim. 32 (2) (2006) 161–167.

[20] M. Kiani, H. Shiozaki, K. Motoyama, Int. J. Veh. Des. (2013) (Epub ahead of print).

[21] M. Kiani, M. Rais-Rohani, K. Motoyama, H. Shiozaki, Proc. IMech Part D: J. Automob. Eng. 228 (6) (2014) 689–700.

[22] B. Paramjot, D. Metin, G. Moore, et al., in: Proceedings of MSC 1996 World Users' Conference, IV(34), 1996.

[23] S. Donders, M. Brughmans, L. Hermans, C. Liefooghe, H.V. Auweraer, W. Desmet, et al., Fin. Elem. Anal. Des. 42 (2006) 670–682.

[24] K.K. Mustafa, Int. J. Adv. Manuf. Technol. 39 (2008) 851–865.

[25] F. Chen, T. Huang, J. Mater. Process Technol. 142 (2003) 643–647.

[26] LS-DYNA Keyword User's Manual, Material Models, vol. 2, 2012, pp. 529–532. Rev. 1196, Version 971.

[27] D.A. Wagner, S.D. Logan, K. Wang, T. Skszek, et al., in: Proceedings of the SAE 2010 World Congress & Exhibition, Detroit, MI, 2012.

[28] A. Najafi, M. Rais-Rohani, Thin wall Struct. 49 (2011) 1–12.

[29] T.W. Simpson, J. Peplinski, P.V. Koch, K.J. Allen, et al., Eng. Comput. 17 (2001) 129–150.

[30] E. Acar, M. Rais-Rohani, Struct. Multidiscip. Optim. 37 (2008) 279–294.

[31] E. Acar, K. Solanki, Int. J. Crashworthiness 14 (2009) 49–61.

[32] U.M. Diwekar, J.R. Kalagnanam, AICHE J. 43 (1997) 440–447.

[33] R.L. Hardy, J. Geophys. Res. 76 (1971) 1905–1915.

[34] M.J.D. Powell, in: J.C. Mason, M.G. Cox (Eds.), Algorithms for Approximation, Oxford University Press, London, 1987, pp. 143–167.

[35] A. Serna, C. Bucher, Advanced Surrogate Models for Multidisciplinary Design Optimization, 2009. Presented at the 6th Weimar Optimization and Stochastic Days.